

Research Paper

# Vandetanib-eluting Radiopaque Beads: *In vivo* Pharmacokinetics, Safety and Toxicity Evaluation following Swine Liver Embolization

Alban Denys<sup>1</sup>, Peter Czuczman<sup>2</sup>, David Grey<sup>2</sup>, Zainab Bascal<sup>2</sup>, Rhys Whomsley<sup>2</sup>, Hugh Kilpatrick<sup>2</sup>, Andrew L. Lewis<sup>2</sup>✉

1. Department of Radiology and Interventional Radiology, CHUV University of Lausanne, Lausanne, Switzerland;

2. Biocompatibles UK Ltd, a BTG International group company, Lakeview, Riverside Way, Watchmoor Park, Camberley, GU15 3YL, UK.

✉ Corresponding author.

© Ivyspring International Publisher. This is an open access article distributed under the terms of the Creative Commons Attribution (CC BY-NC) license (<https://creativecommons.org/licenses/by-nc/4.0/>). See <http://ivyspring.com/terms> for full terms and conditions.

Received: 2017.02.14; Accepted: 2017.04.04; Published: 2017.06.01

## Abstract

**PURPOSE:** To evaluate the plasma and tissue pharmacokinetics, safety and toxicity following intra-arterial hepatic artery administration of Vandetanib (VTB)-eluting Radiopaque Beads (VERB) in healthy swine.

**MATERIALS AND METHODS:** In a first phase, healthy swine were treated with hepatic intra-arterial administration of VERB at target dose loading strengths of 36 mg/mL (VERB36), 72 mg/mL (VERB72) and 120 mg/mL (VERB120). Blood and tissue samples were taken and analysed for VTB and metabolites to determine pharmacokinetic parameters for the different dose forms over 30 days. In a second phase, animals were treated with unloaded radiopaque beads or high dose VTB loaded beads (VERB100, 100 mg/mL). Tissue samples from embolized and non-embolized areas of the liver were evaluated at necropsy (30 and 90 days) for determination of VTB and metabolite levels and tissue pathology. Imaging was performed prior to sacrifice using multi-detector computed tomography (MDCT) and imaging findings correlated with pathological changes in the tissue and location of the radiopaque beads.

**RESULTS:** The peak plasma levels of VTB ( $C_{max}$ ) released from the various doses of VERB ranged between 6.19-17.3 ng/mL indicating a low systemic burst release. The plasma profile of VTB was consistent with a distribution phase up to 6 h after administration followed by elimination with a half-life of 20-23 h. The AUC of VTB and its major metabolite N-desmethyl vandetanib (NDM VTB) was approximately linear with the dose strength of VERB. VTB plasma levels were at or below limits of detection two weeks after administration. In liver samples, VTB and NDM VTB were present in treated sections at 30 days after administration at levels above the *in vitro*  $IC_{50}$  for biological effectiveness. At 90 days both analytes were still present in treated liver but were near or below the limit of quantification in untreated liver sections, demonstrating sustained release from the VERB. Comparison of the reduction of the liver lobe size and associated tissue changes suggested a more effective embolization with VERB compared to the beads without drug.

**CONCLUSIONS:** Hepatic intra-arterial administration of VERB results in a low systemic exposure and enables sustained delivery of VTB to target tissues following embolization. Changes in the liver tissue are consistent with an effective embolization and this study has demonstrated that VERB100 is well tolerated with no obvious systemic toxicity.

Key words: Vandetanib-eluting Radiopaque Beads, pharmacokinetics, safety and toxicity

## Introduction

Drug Eluting Beads (DEBs) are controlled release microspherical devices that are used for sustained locoregional delivery of chemotherapeutic agents to various tumor types [1-4]. As compared with systemic delivery, they are associated with a decrease in the

systemic circulation of the antineoplastic, an increase of drug concentration in target tissue and an extended presence in the tumor [5, 6]. DEBs are finding increasing use in the treatment of hepatic malignancies by intra-hepatic arterial administration

by a procedure known as transarterial chemoembolization (TACE) [7]. This procedure is in itself a combination therapy, which induces oxygen and nutrient deprivation to the tumor by occluding the feeding blood vessels, whilst providing for a concomitant sustained delivery of a high local dose of chemotherapy. DC Bead™ is the most widely studied DEB and is approved for loading with doxorubicin (DEBDOX) for the treatment of patients suffering from hepatocellular carcinoma (HCC, primary cancer originating in the liver) [5, 8-10]; whereas for those suffering from colorectal cancer metastases (mCRC) to the liver, may be treated with DC Bead™ loaded with irinotecan (DEBIRI) [11-15]. It has also been demonstrated that it is possible to administer DEBs by directly injecting them at the diseased site, for instance in pre-clinical animal models of peritoneal carcinomatosis [4], glioblastoma [2, 16] and pancreatic cancer [3, 17], although this is not currently within any of the DEB approval indications.

Although DEBs offer an effective locoregional anticancer treatment with significant reductions in drug-related side effects, the fact remains that in many patients tumor growth will reoccur and their disease will ultimately progress. In an attempt to address this limitation, we explored the possibility of loading DEBs with newer small-molecule antitumor agents which have been designed to specifically target motifs on or within tumor cells in order to block signalling for pro-survival pathways that are responsible for cancer cell proliferation, angiogenesis and metastasis. For instance, the multi-target kinase inhibitor (MTKi) sorafenib that targets both RAF and vascular endothelial growth factor receptor (VEGFR), improves overall survival of advanced HCC patients [18, 19] and is now the recommended treatment in this population. The inhibitor of epidermal growth factor receptor (EGFR) erlotinib, has shown modest anti-tumor effects in patients with advanced HCC [20]. There is in general however, a significant issue of adverse side effects related to the systemic exposure of these types of agents [21-23] and therefore intra-arterial delivery from a DEB could be a feasible approach. Sunitinib has been successfully loaded into DC Bead™ [24, 25] and although significant antitumoral efficacy of the Sunitinib-eluting Beads was observed in the VX2 rabbit tumor model [26], serious issues concerning systemic toxicity of sunitinib (18.5% death due to drug toxicity) [27] has led to exploring alternative candidates.

Vandetanib (VTB) is a MTKi targeting both VEGFR and EGFR, approved for the treatment of advanced medullary thyroid cancer [28-31]. It binds covalently to the cysteine residues of the TK domain

and prevents binding of ATP, phosphorylation of the TK dimer and initiation of subsequent downstream signalling pathways. Xenograft studies confirm that VTB has activity across a number of different tumor types as a single agent in the dose range 25-50 mg/kg [32] and the drug recently demonstrated a good safety profile but limited efficacy compared to placebo in HCC [33]. In a randomized, double-blind, parallel group, multi-center, phase II study to assess the efficacy and safety of either 100 mg or 300 mg daily oral dose of VTB *versus* best supportive care (BSC) in patients with inoperable HCC, there were no significant differences in tumor stabilization rate (total of complete response, partial response and stable disease rates after 16 weeks), although there was some suggestion of a possibility of a benefit in overall survival. There were however, significant adverse events including diarrhoea, rash, GI haemorrhage and QT prolongation associated with the systemic exposure, which might be overcome by DEB delivery. We have recently reported on the preparation and characterization of a Vandetanib-eluting Radiopaque Bead (VERB) [34], which has also demonstrated efficacy in the VX2 tumor model (unpublished data). Here we report on the pharmacokinetics and safety of a preloaded version of VERB in a healthy swine liver embolization model, in preparation for first in human clinical evaluation.

## Materials and Methods

### Vandetanib-eluting Radiopaque Bead Preparation

Vandetanib API (VTB, AstraZeneca, UK) was dissolved at approximately 20 mg/mL in hydrochloric acid (0.1 M) to aid the solubilization of the drug. 1.2 mL of Radiopaque Beads (ROB) [35] (Biocompatibles UK Ltd, Farnham, UK) was dispensed into a 10 mL glass vial (SCHOTT, Type 1), the packing solution was removed and beads were loaded with target doses of 36, 72 or 120 mg VTB using the appropriate volume of the stock solution. Drug loading was performed with shaking for 2 hrs for 36 and 72 mg samples, and overnight for 120 mg samples. Loading dose was determined by washing the beads with purified water and analysing the washing solution by HPLC. 1 mL of purified water was added to the drug loaded beads and the beads were frozen at -20°C for approximately 2 hours. Loaded beads were lyophilized overnight in a benchtop freeze-drier (Heto Drywinner). The lyophilized beads were sealed with rubber bungs (Bromobutyl stopper, Daikyo), crimped and gamma sterilized at 25 kGy dose (Synergy Health).

## Size Characterization of Vandetanib-eluting Radiopaque Beads

The lyophilized beads were hydrated with 1.5 mL purified water and left for 30 minutes to hydrate. The volume of beads was determined by transferring them to a 5 mL measuring cylinder and reading the sedimented volume. Bead morphology was observed under an Olympus BX50 optical microscope at X 10 magnification. The diameter of 200 beads per vial was measured.

## Hepatic Arterial Embolization with Vandetanib-eluting Radiopaque Beads

This evaluation was performed in a swine liver embolization safety model [36, 37] at MPI Research Inc. (Mattawan, Michigan, USA) using male experimentally naïve domestic Yorkshire crossbred swine (farm pigs, weights 53.5 - 66.5 kg at randomization). The study conformed to USDA Animal Welfare Act (9 CFR parts 1, 2 and 3) and the 'Guide for the Care and Use of Laboratory Animals', Institute of Laboratory Animal Resources, National Academy Press, Washington, D.C, 2011.

### Study Design

This study was designed in two phases: a 30 day study to evaluate pharmacokinetics and tissue levels of drug from three different dose levels of beads, and a second phase designed to look at histopathology, imaging and tissue levels at 90 days from one fixed dose (Table 1). For phase one, when the animal was administered with the full 1 mL dose volume of beads the actual dose of VTB was either: 36 mg, 72 mg, or 120 mg. These groups were denoted as VERB36, VERB72 and VERB120 and three randomized animals were treated per group. Delivery of up to 1 mL of beads was anticipated to achieve near-stasis of a third to a half of the liver volume. The final volume delivered was based upon intra-procedural imaging feedback obtained during the administration procedure.

**Table 1.** Outline of the two study phases

Group	Phase One Study 30 Days				Phase Two Study 30/90 days	
	OVTB	VERB36	VERB72	VERB120	ROB	VERB100
Target Drug Dose (mg)	31,500	36	72	120	0	100
Mean Bead Diameter (µm)	NA	93.1	91.7	92.4	94.7	84.9
Number of Animals	3	3	3	3	3/3	4/4

An oral gavage group (OVTB) was included to allow for pharmacokinetic comparison of the current clinical route for VTB therapy (oral route) *versus*

intra-arterial delivery of drug loaded beads (n=3). A dose level of 21 mg/kg/day was selected based upon allometry, as this was predicted to provide drug plasma levels similar to those seen for humans receiving a 300 mg clinical dose *via* oral route [38].

For phase two, animals were treated with either the unloaded radiopaque bead (ROB, n=6) or VTB-beads loaded with 100 mg/mL (denoted VERB100, n=8). At 30 days post administration, half of the animals in each group were imaged using Multi-Detector Computed Tomography (GE VCT Slice CT scanner) and then sacrificed in order to undertake histopathology analysis and tissue drug and metabolite levels. Imaging characteristics were as follows: 1.3 mm slice thickness, 300 mA, 120 kV and field of view 36 x 36 cm. The same process was repeated for the remaining half of the groups at 90 days post administration.

### Swine Hepatic Embolization Procedure

The vial of lyophilized beads was rehydrated in 4mL of sterile water, gently swirled and left for 30 minutes to rehydrate. The beads were mixed 1:19 with Omnipaque 350™ and suspended by transferring between two syringes through a 3-way stopcock. Bead suspension was aliquoted into a 3mL syringe for delivery through the microcatheter to allow for better control and re-suspended regularly to prevent sedimentation.

A sheath was placed (Avanti 7F) in the femoral artery of the pig and under fluoroscopic guidance using an OECD 9900 Fluoroscope, a radio-opaque guidewire (Luge™ 0.014" x 182 cm (Boston Scientific Corp.) or Emerald® 0.35 inches (Cordis Corp.) was passed through the introducer into the femoral artery. A 4 Fr Cobra 2 catheter (AngioDynamics Inc.) was then positioned in the celiac axis and a celiac angiogram obtained by injecting contrast media. A 2.7 Fr microcatheter (Progreat®, Terumo Japan) was then advanced in the hepatic artery branch chosen because it fed around 50% of the liver volume. The guidewire was subsequently removed and contrast media was used to capture an angiogram of the lobe(s). With the catheter in position and an appropriate target location identified, the test article was administered slowly under continuous fluoroscopy, evaluating changes in vascular flow rate and appearance of reflux or non-target embolization of the beads (inferred from visible contrast flow).

The bead suspension was slowly administered under fluoroscopic guidance until the maximum volume was administered for all animals. Dosing occurred in the left lateral lobe or left median lobe for all animals. At the end of the embolization, bead suspension remaining within the micro-catheter was

flushed with saline prior to removing the micro-catheter. Pre- and post-embolization DSA images were used to document embolization effect (Table 2). Output cine fluoro loops and angiograms were used to assess the extent of embolization. Vascular flow was graded post-embolization to cover the range from complete occlusion to non-occlusion as indicated in Table 2. After all images were obtained, all guides, catheters, and the sheath were removed. The femoral artery was ligated. The muscle and subcutaneous tissues were closed with absorbable suture, and the skin was closed with skin glue. Vascular access site observations were performed daily up to Day 8 following intervention for signs of infection, inflammation, and general integrity.

**Table 2.** Outcome of bead embolization procedures

Group	Study	Vascular Flow Score*	Average Bead Suspension Delivered (mL)	Average Sedimented Bead Volume Delivered (mL)	Average Drug Dose Administered (mg)
VERB36	Phase One	2(3)	18.833	0.94	30.9
VERB72	Phase One	1(2), 2(1)	16.333	0.82	58.8
VERB120	Phase One	1(3)	19.167	0.96	115.0
ROB	Phase Two	1 (3), 2(3)	20.000	1.0	NA
VERB100	Phase Two	1(6), 2(2)	19.538	0.98	97.7

\* (1=slow antegrade flow in the embolized artery beyond the point of obstruction without perfusion distal to the occlusion; 2= slow antegrade flow in the embolized artery beyond the point of obstruction with partial perfusion or full perfusion with slow flow distal to the occlusion; Number in brackets = number of animals with this score)

## Clinical Observations and Measurements

A detailed clinical examination of each animal was performed at receipt, prior to randomization, and daily during the study. All animals were observed for morbidity, mortality, injury, and the availability of food and water twice daily. Body weights for all animals were measured and recorded at receipt, prior to randomization, and weekly during the study. Ophthalmoscopic examinations were conducted pre-test and prior to sacrifice and electrocardiographic monitoring was performed pre-test, throughout the procedure, 1 hour post administration, 20 hours post recovery from surgery and for 20 hours a few days prior to sacrifice.

## Investigation of Vandetanib and Metabolite Plasma Pharmacokinetics and Tissue Concentrations

Blood samples (approximately 1 mL) were collected from all animals in phase one *via* the jugular or other suitable vein for determination of the plasma

concentrations of the test article, vandetanib (VTB), and the metabolites, N-desmethyl vandetanib (NDM VTB) and vandetanib N-oxide (VTB-NO). Concentrations of an unknown metabolite were also investigated. Samples were collected pre-test, 5 and 20 minutes post-dose, and 1, 2, 6, 24, 72 hours post-dose on Day 0, and once on Days 5, 7, 14, 21, and 29. Projected collection times for embolized animals were based on the completion time of dosing (after flush). The animals were not fasted prior to blood collection, with the exception of the intervals that coincided with fasting for clinical pathology collections. Samples were placed in tubes containing lithium heparin as an anticoagulant. The blood samples were collected on ice and centrifuged under refrigeration. Plasma samples were stored frozen at -60 to -90°C until analysis (York Bioanalytical Solutions Ltd., United Kingdom).

Liver sections (approximately 3 x 5 g each) were collected from each liver lobe (treated and untreated areas where treatment was with embolization) for determination of the tissue concentrations of the test article and the metabolites. High resolution X-ray images were used to collect the representative samples from the treated areas of the liver. The samples from the treated lobe were taken and identified as proximal, middle, and distal to the approximate area of bead administration. The samples from the untreated lobes were taken and identified in a similar manner (i.e., proximal was the approximate area where the main arterial blood supply entered that lobe, distal was taken from the periphery of the lobe, and the middle area sample was taken mid-way between the other two samples). The samples were wrapped in foil and snap frozen in liquid nitrogen. The samples were labeled with the animal number and the liver lobe identification. The tissue samples were stored frozen at -70 to -90°C until shipped on dry ice to York Bioanalytical Solutions Ltd., United Kingdom, for analysis.

VTB, VTB-NO and NDM VTB metabolite concentrations in swine plasma and liver were determined using solid phase extraction followed by liquid chromatography (Acquity iClass/Shimadzu Nexera) coupled to tandem mass spectrometry (MDS API5000) using turbospray in positive ion, multiple reaction monitoring mode. Separation was achieved using a 5 mL injection into a Thermo Accucore HILIC 50 x 3 mm 2.6 µm analytical column run at 40°C, using formic acid (0.2 %) in acetonitrile: water: ammonium formate (1 M) mobile phases at 0.6 mL/min. VTB together with various metabolites and labelled analytical/internal standards (purity 99.1 - 100 %, AstraZeneca) were used as reference standards for the chromatography.

Individual VTB, NDM VTB, unknown metabolite, and VTB-NO concentration-time profiles from OVTB, VERB36, VERB72, or VERB120-treated animals were analyzed using model-independent methods. Toxicokinetic parameters were obtained for each animal following the first dose administration. Concentrations less than the lower limit of quantitation (LLOQ < 0.100 ng/mL) were reported as and set to zero in the calculations. Nominal times were used for toxicokinetic data analysis. For each animal, the following toxicokinetic parameters were determined: maximum observed plasma concentration ( $C_{max}$ ), time of maximum observed plasma concentration ( $T_{max}$ ), and area under the plasma concentration-time curve (AUC). The AUC from time 0 to 24 hr ( $AUC_{0-24hr}$ ) and from time 0 to the time of the final quantifiable sample ( $AUC_{Tlast}$ ) were calculated by the linear trapezoidal method for all animals with at least three consecutive quantifiable concentrations. Half-life values ( $T_{1/2}$ ) were reported for individual plasma concentration-time profiles that had sufficient plasma concentrations in the terminal elimination phase (at least three samples not including  $T_{max}$ ) and an adjusted  $R^2$  of  $\geq 0.9$ . Additional toxicokinetic parameters calculated were clearance (CL/F), and volume of distribution ( $V_z/F$ ). The fraction of dose absorbed (F) was not determined; therefore  $V_z/F$  and CL/F were not normalized for the fraction of dose absorbed.

### Evaluation of Vandetanib-eluting Radiopaque Bead Imaging

Thirty day post-embolization CT scans were performed on Phase One animals without administration of IV contrast and were available for review for all twelve animals. In Phase two, CT scans were performed on all animal after administration (Day 0) and prior to necropsy (Either Day 30 or 90). CT images from both phase one and two studies were analyzed to document location, distribution and level of radiopacity of the embolized beads. Specifically, the CT scans were reviewed for the following: i) CT visibility of unloaded and drug loaded beads, ii) distribution of beads within the liver, iii) approximate area/volume of liver embolized, and iv) extrahepatic non target embolization in adjacent organs including the stomach, spleen, pancreas and small bowel, specifically the duodenum, and in the visualized lungs.

### Pathological Analysis of the Effects of Vandetanib-eluting Radiopaque Bead

Necropsy examinations were performed on the phase two animals under procedures approved by a veterinary pathologist on animals at the scheduled

necropsies (Day 30 and Day 90). The animals were euthanized by an intravenous injection of sodium pentobarbital solution under Telazol® sedation, followed by exsanguination *via* transection of the femoral vessels. The animals were examined carefully for external abnormalities including palpable masses. The skin was reflected from a ventral midline incision and any subcutaneous masses were identified and correlated with antemortem findings. The abdominal, thoracic, and cranial cavities were examined with special attention paid to the liver, associated vasculature, surrounding tissues, gallbladder, hepatic bile ducts, gastrointestinal tract, lungs, heart, kidney, spleen, and brain for abnormalities. The organs were removed, examined, and, where required, placed in fixative for subsequent analysis for tissue abnormalities and off-target embolization. All designated tissues were fixed in neutral buffered formalin. The liver was submitted for high resolution X-ray prior to sectioning to aid in identification of the treated lobe. Microscopic examination of fixed hematoxylin and eosin-stained paraffin sections was performed on protocol-designated sections of tissues. Three sections of treated liver were examined for all animals. The slides were examined by a board-certified veterinary pathologist. Special stains were used by the pathologist as needed to aid in the diagnosis of specific lesions and representative photomicrographs of tissue sections were taken.

## Results

### Embolization Procedure with Vandetanib-eluting Radiopaque Beads

In the phase one study VERB36, VERB72, or VERB120 beads were successfully delivered under fluoroscopic guidance until near stasis was achieved or angiographic evidence of the potential for extra-hepatic non target embolization was observed. Almost the entire dose was administered to all animals with the exception of animal in the VERB72 group that received just 10 mL of volume (out of 20 mL total) as the embolization was stopped due to angiographic evidence of the potential for extra-hepatic non-target embolization (Table 2). During administration, there was no evidence of beads settling or clogging within the catheter, extra-hepatic non-target embolization, or reflux exceeding 1 to 2 cm from the catheter tip. Following completion of embolization, vascular blood flow within the treated lobe of the liver was assessed to evaluate level of vascular occlusion.

There were no abnormal clinical observations or vascular access site observations related to administration of the test article. The clinical findings

observed (e.g., abrasions, scabbed areas, lacrimation) are commonly seen in animals of this sex, age, and species. There were no test article-related body weights effects evident. Animals across all groups gained a similar percentage of weight (9 to 16%) during the course of the study from Week 1 until study termination (Week 4 or 5). VTB has some reported adverse effects on the eyes (corneal verticillata) and the heart (QTc prolongation and cardiac failure) [39] but here there were no abnormal ophthalmoscopic findings evident prior to necropsy and ECG parameters and heart rate were comparable across all groups.

### Investigation of Vandetanib and Metabolite Plasma Pharmacokinetics

Plasma samples from the phase one study were successfully analyzed for concentrations of VTB, NDM VTB and VTB-NO. An unknown metabolite peak was also observed in the analysis, this peak had the same ion transition as VTB-NO and appeared to be present at levels well in excess of the N-oxide metabolite but is not reported in this analysis. This metabolite has not been reported in humans, mice or rats but has been observed during this study in swine and also in rabbits (unpublished data). Pharmacokinetic parameters were calculated for VTB, NDM VTB and VTB-NO and are shown in Table 3. Figure 1(a) shows that the  $T_{max}$  (time to reach  $C_{max}$ ) is achieved within approximately 1 hour of treatment administration for the VERB groups and approximately 2 hours for OVTB given the dose difference (21 mg/kg). Figure 1(b) shows that the values of the area under the curve (levels of drug in

the plasma over time) measured after either 24 hours ( $AUC_{0-24}$ ) or until the last quantifiable measurement was made ( $AUC_{Tlast}$ ), are linearly correlated for both VTB and NDM VTB with the dose of VTB administered in the beads.

### Investigation of Vandetanib and Metabolite Tissue Concentrations

Liver samples collected from the phase one study were successfully analyzed for concentrations of VTB, NDM VTB and VTB-NO (Table 4). The concentrations observed in all OVTB samples for VTB, and four OVTB samples for NDM VTB were reported as >75000 ng/g. These samples were analyzed with a dilution of 500-fold and it was beyond the scope of the validated range to increase the dilution further.

From the phase two study, liver samples from the VERB100 group were successfully analyzed for concentrations of VTB, NDM VTB and VTB-NO (Table 5).

### Imaging Appearance of Embolized Livers

All radiopaque beads, regardless of drug dose, administered during both the phase one and two studies were visible on fluoroscopy and DSA post embolization and contrast wash-out (Figure 2), and on CT (given their high attenuation) both with and without contrast. There was no detectable difference in visibility between the drug loaded bead groups at the three different drug concentrations in the phase one study (Figure 3). In all cases the beads could be seen in hepatic arteries within the embolized lobes, with relatively distal penetration consistent with the size of the beads and lack of proximal aggregation.

**Table 3.** Pharmacokinetic parameters for the Phase One Study

Group	N	$C_{max}$ (ng/mL)	$C_{max}/Dose$ (kg*ng/mL/mg)	$T_{max}$ (hr)	$AUC_{0-24hr}$ (hr*ng/mL)	$AUC_{0-24}/Dose$ (hr*kg*ng/mL/mg)	$AUC_{Tlast}$ (hr*ng/mL)	Cl/F (mL/hr/kg)	$V_z/F$ (mL/kg)	$T_{1/2}$ (hr)
<b>VTB</b>										
OVTB	3	216 ± 33.0	10.3 ± 1.57	2 (2-6)	2860 ± 488	136 ± 23.2	48,300 ± 6670	NA	NA	NA
VERB36	3	6.19 ± 1.56	11.3 ± 3.03	1 (1-1)	72.8 ± 14.4	132 ± 21.6	143 ± 33.4	3780 ± 637	106,000 ± 18,100	19.7 ± 3.95
VERB72	2	15.8 (NA)	13.7 (NA)	(1-2)	174 (NA)	151 (NA)	312 (NA)	3690 (NA)	120,000	22.6 (NA)
VERB120	3	17.3 ± 3.65	8.63 ± 1.74	1 (1-1)	246 ± 68.5	123 ± 37.7	501 ± 185	4320 ± 1480	130,000 ± 29,700	21.5 ± 2.87
<b>NDM VTB</b>										
OVTB	3	126 ± 25.3	6.02 ± 1.2	696 (504-696)	417 ± 45.9	19.9 ± 2.18	51,800 ± 5040	NA	NA	NA
VERB36	3	0.565 ± 0.146	1.03 ± 0.304	24 (24-24)	7.86 ± 0.976	14.3 ± 2.30	40.9 ± 4.35	NA	NA	NA
VERB72	2	0.951 (NA)	0.824 (NA)	(24-72)	16.2 (NA)	14.1 (NA)	89.7 (NA)	11,800 (NA)	824,000 (NA)	48.5 (NA)
VERB120	3	1.69 ± 0.254	0.843 ± 0.150	24 (24-24)	23.0 ± 5.23	11.5 ± 2.93	151 ± 46.6	12,800 ± 4020	818,000 ± 301,000	43.7 ± 5.52
<b>VTB-NO</b>										
OVTB	3	1.35 ± 0.259	0.0643 ± 0.0124	2 (2-2)	15.4 ± 0.739	0.732 ± 0.0352	246 ± 32.1	NA	NA	NA
VERB36	3	0.154 ± 0.02	0.282 ± 0.0468	0.083 (0.083-0.333)	NA	NA	0.317 (NA)	NA	NA	NA
VERB72	2	0.384 (NA)	0.329 (NA)	(0.083-2)	NA	NA	0.404 (NA)	NA	NA	NA
VERB120	3	0.374 ± 0.065	0.186 ± 0.0345	0.083 (0.083-0.083)	NA	NA	1.2 ± 0.576	NA	NA	1.0 ± 3.39

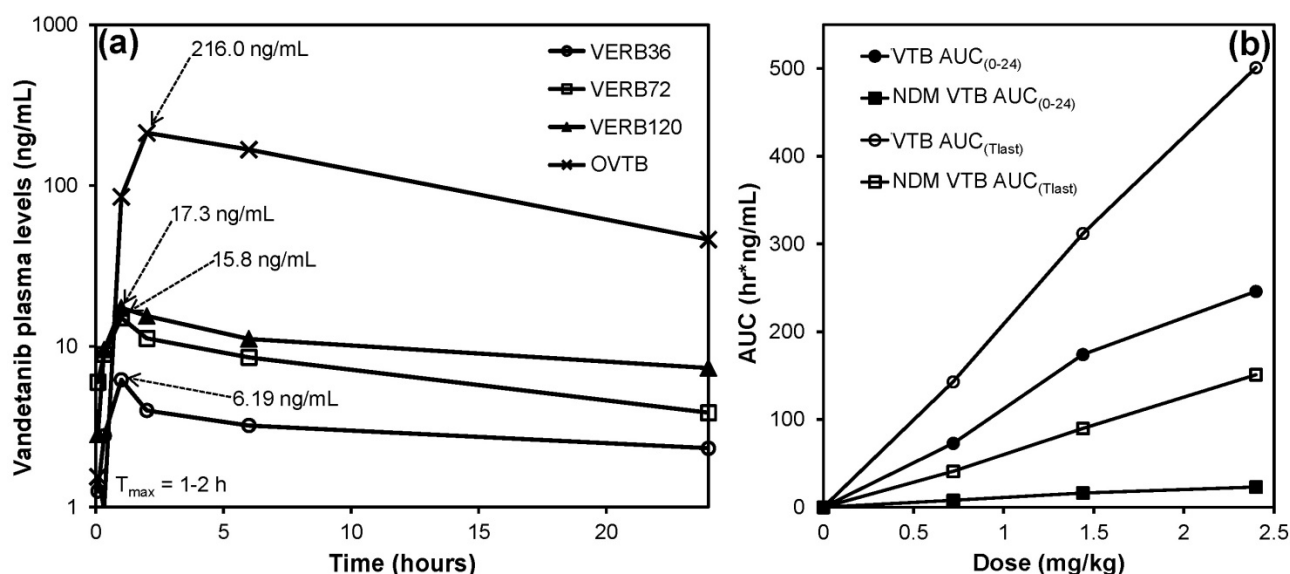


**Figure 1.** (a) Plasma levels of VTB for the first 24 hours following treatment with OVTB, VERB36, VERB72 and VERB120; (b) Areas under the curve (AUC) between T=0 and 24 hours (AUC<sub>(0-24)</sub>) and T=0 and the last quantifiable data point (AUC<sub>(Tlast)</sub>) for VTB and NDM VTB versus VTB dose administered. (Error bars are omitted for clarity, see Table 3 for standard deviations).

**Table 4.** Analyte concentrations in liver samples from the phase one study (taken from embolized and non-embolized regions for the bead-treated groups) at day 30 post-embolization. Data shown are the mean with the range in brackets.

Group	Analyte Concentration (ng/g) in Liver Sample Section 30d					
	VTB		NDM VTB		VTB-NO	
OVTB (n=6)	>75,000					
	Embolized (n=3)	Non-embolized (n=3)	Embolized (n=3)	Non-embolized (n=3)	Embolized (n=3)	Non-embolized (n=3)
VERB36	103.0 ± 124.2	47.1 ± 64.9	63.4 ± 96.7	35.1 ± 48.0	0.255	<LLOQ
VERB72	34.5 ± 42.2	4.54 ± 2.7	3.15 ± 2.05	3.68 ± 1.90	0.239	<LLOQ
VERB120	167.0 ± 158.8	2.86 ± 0.6	6.26 ± 3.16	1.91 ± 0.63	1.61	<LLOQ

(BLQ=Below Lower Limit of Quantification; <LLOQ = <Lower Limit of Quantification (0.150))

**Table 5.** Analyte concentrations in liver samples from the phase two study (mean of the three liver locations, ±SD), embolized and non-embolized regions treated with VERB100 at day 30 and 90 post-embolization (NA= not applicable).

Analyte	30 Days		90 Days	
	Embolized (n=12)	Non-embolized (n=12)	Embolized (n=9)	Non-embolized (n=9)
VTB	105.8 ± 249.1	0.585 ± 0.222	8.55 ± 7.84	0.121 ± 0.106 (n=4)
NDM VTB	6.31 ± 8.01	0.478 ± 0.180	1.73 ± 1.67	NA
VTB-NO (n=8)	0.640 ± 0.961	NA	NA	NA

In the phase two study, all animals administered with control or VERB100 bead suspension received greater than 92% of the full dose prepared for administration (dose volume ranging from 18.5 to 20 mL). By fluoroscopic estimation, approximately 50 % of the liver volume was embolized in all animals. There was also no definitive difference in the distribution of the beads in the embolized liver. The

appearance did not change from the Day 0 to the Day 30 or Day 90 repeat CT examinations (Figure 4).

No biliary ductal dilatation was noted on the Day 0 CTs of unloaded or drug loaded beads with targeted lobe sizes similar between both. Biliary dilatation was seen on 4/4 Day 30 CTs of the VERB100 group and 0/3 the Day 30 CTs of the ROB control group. The Day 90 CTs of the VERB100 group show 2/3 with biliary dilatation. The Day 90 CTs of the unloaded control group show 2/3 with biliary dilatation. Lobe size of both control group and VERB100 group were compared to initial appearance and adjacent non-targeted lobes. There was a reduced size of the targeted lobe in 6/7 VERB100 group (Figure 5(b)). The control group demonstrated decreased size in 0/6. This was noted to be present on Day 30 and Day 90 CTs. Areas of decreased perfusion on initial CT demonstrate decreased size on follow up CT. Again, the finding can be attributed to more effective embolization which would decrease lobule and hence lobe size.

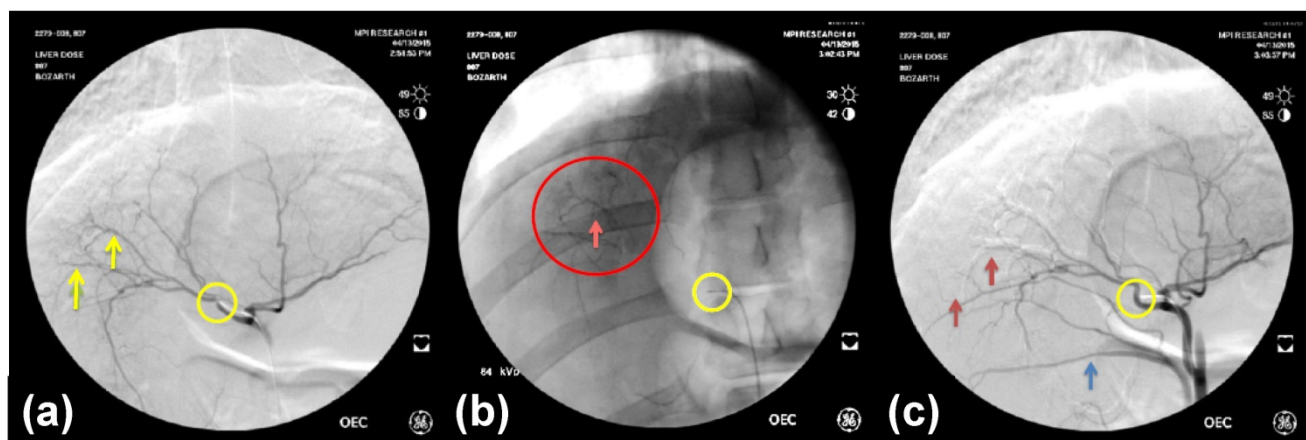


**Figure 2.** (a) DSA pre-embolization showing arteries to be embolized (yellow arrows); (b) Fluoroscopic image post-embolization and contrast wash-out showing VERB100 in arteries (red circle); (c) DSA post-embolization showing shadowing imaging artefact from the radiopaque beads in the arteries (red arrows). Catheter tip position is shown in the yellow circle and the blue arrow points to reflux of contrast in a more proximal arterial branch related to distal embolization.

### Pathological Findings following Embolization

Injected beads were present in sections of treated liver in all animals of the phase two study groups, with no beads seen in the untreated sections of liver. Changes were mostly segmental affecting only portions of the sections examined, with beads being more abundant in the intermediate and distal sections compared to the proximal sections of treated liver. After staining and processing, the beads appeared as deep blue spheres present in small vessels in portal spaces. Occasionally the beads were displaced from the tissue during sectioning, leaving a round hole in the section where they were previously located (e.g. Figure 6 (d)).

Interlobular fibrosis was observed for both unloaded (1/3 animals, Figure 6(a)) and the VERB100 group (4/4 animals, Figure 6(b)) at 30 days and this persisted at 90 days (3/3 and 2/3 animals respectively). This was often associated with bile duct hyperplasia, encircling lobules that were reduced in size, resulting in a macroscopic reduction in the size of the treated liver lobe (Figure 6(b, c)). Reduced lobule size in the treated sections of liver in the VERB100 group (3/4 animals) was characterized by smaller lobules with disorganized trabeculae but no evidence of hepatic degeneration. The finding correlated to the reduced lobe size noted following radiologic evaluation (Figure 5(b)). The shrunken lobules were lined by small bile ducts extending from the portal spaces (identified as bile duct hyperplasia, 3/4 animals) and/or variably sized bundles of fibrosis (interlobular fibrosis, 4/4 animals, Figure 6(c)). In addition, large bile ducts were occasionally dilated (Figure 6(b)) and were surrounded or had inflammatory infiltrate in their lumen (2/4 animals, Figure 6(d)). The bile duct dilation was also noted

following radiologic evaluation (Figure 5(b)). None of these treatment-related findings were present in the untreated liver section and are consistent with impaired blood flow with subsequent necrosis and regeneration.

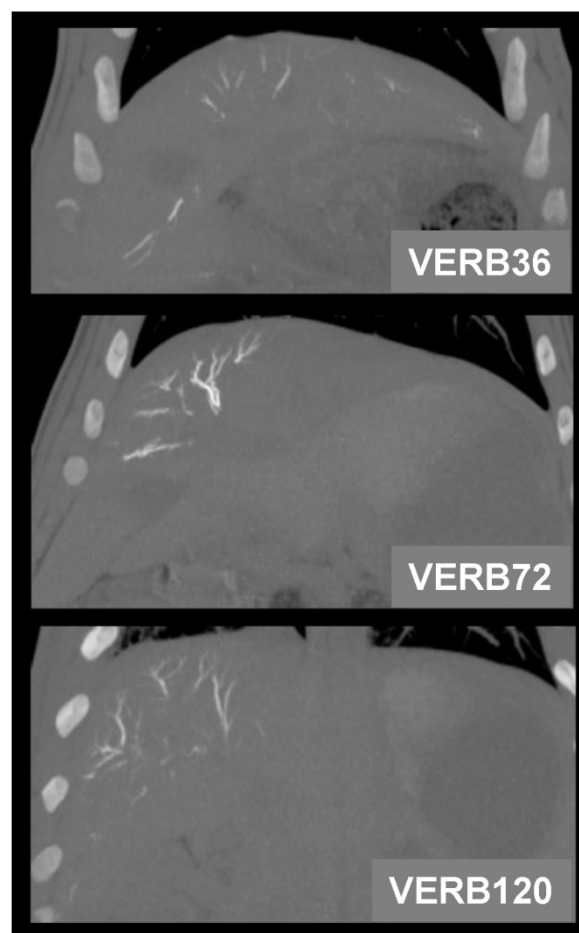


**Figure 3.** 30 Day coronal thin MIP reformations from CT acquisition showing the distribution of beads in one representative animal per group. There is no difference in CT visualization or density between VERBs of different drug doses.

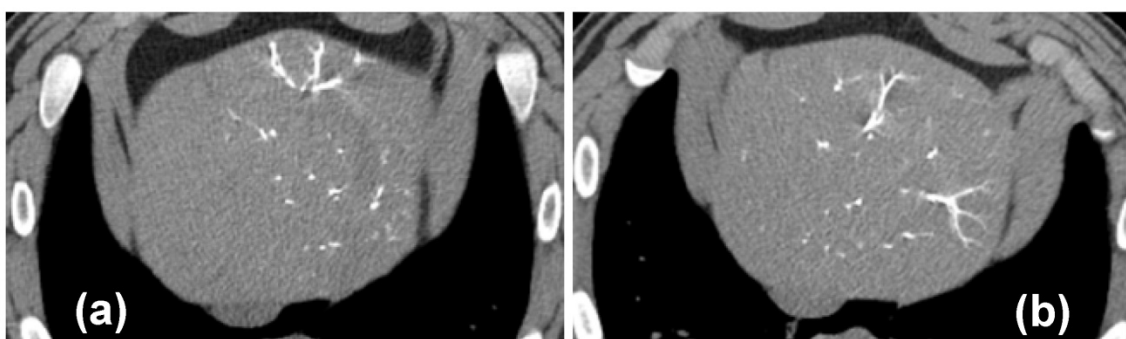


**Figure 4.** MDCT axial images of the liver of VERB100 treated animals at (a) 1 hour post-embolization and (b) 90 Days post-embolization, showing no discernible differences in bead visibility.

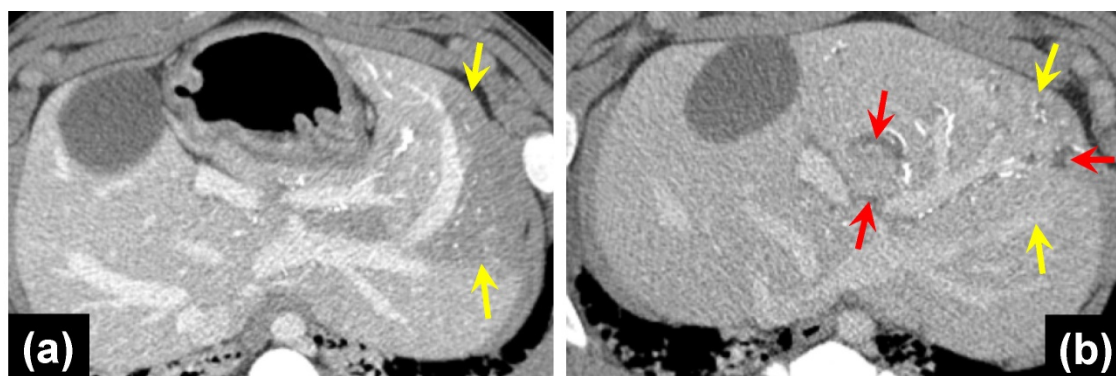


**Figure 5.** (a) MDCT axial image of portal venous phase post contrast, 1 hour post-embolization with VERB100, yellow arrows point to areas of decreased hepatic parenchymal enhancement; (b) MDCT axial image of portal venous phase post contrast, red arrows indicate dilated bile ducts, yellow arrows show the reduced left liver lobe size 30 days post-embolization.

On day 90 of the phase two study, interlobular fibrosis (3/3 animals), reduced lobule size (3/3 animals), and/or bile duct hyperplasia (2/3 animals) were present in the treated liver of the unloaded control group. The interlobular fibrosis was present in the treated liver sections of all the unloaded control group animals compared to only one animal on day 30 of the study (Figure 7(a)). The interlobular fibrosis was associated with bile duct hyperplasia and/or decreased lobule size in the unloaded control group and similar to what was observed on day 30 in the VERB100 group. The reduced lobule size and bile duct dilatation/ inflammation were resolved in the treated liver sections in the VERB100 group, whereas bile duct hyperplasia (2/3 animals) and interlobular fibrosis (2/3 animals) although less severe, were still present in the treated sections compared to the untreated liver (Figure 7(b-d)).

## Discussion

Hepatic arterial embolization using VERB was shown to be feasible and safe. For the pharmacokinetic evaluation of VTB and metabolites in the plasma, it was observed that there was a surprisingly low burst release of VTB in the first hours post-administration ( $C_{max}$  ranging from 6.19-17.3

ng/mL for the three doses). Assuming a blood volume of around 3.9 L in a 60 kg animal and minimal metabolism and elimination in the first hour, this represents <0.1 % of the loaded drug dose on the VERB. The normalized  $AUC_{0-24hr}$  of the different VERB dose groups in phase one were 136, 132, 151, and 123  $hr \cdot kg \cdot ng/mL/mg$ , respectively. This indicates a linear relationship between dose and  $AUC_{0-24hr}$  for all groups assuming that the oral dose is completely absorbed. The  $AUC_{Tlast}$  also showed a linear relationship with dose for the VERB groups. The mean elimination half-life values were very similar for the VERB groups at 19.7, 22.6, and 21.5 hr respectively, illustrating that the drug is eliminated slowly and has good opportunity to accumulate to effective levels in the targeted tissues. The same linear trend in  $AUC$  versus dose was also evident for the NDM VTB metabolite. The long  $T_{max}$  for this metabolite in the OVTB group suggests that it accumulates on repeated administration which is consistent with its long half-life where measurable. The NDM VTB metabolite has similar inhibitory activity against VEGFR-1, VEGFR-2, EGFR and FGFR-1 compared to the parent compound, VTB-NO to a much lesser extent. [40] and the long-lived nature of these metabolites in the target tissue is useful from a locoregional efficacy perspective.

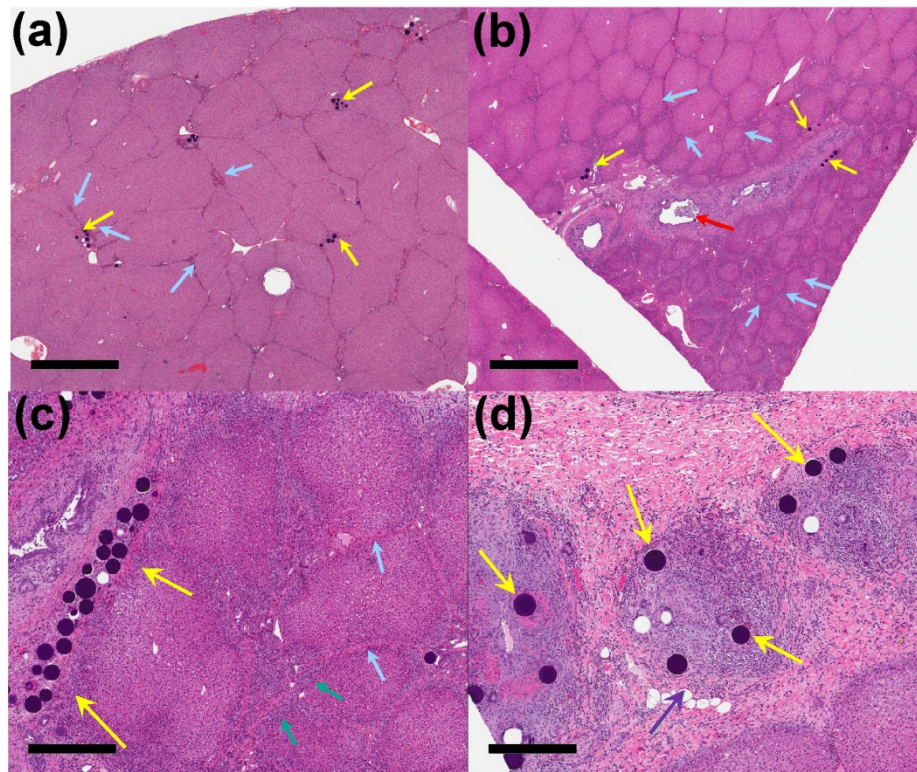


**Figure 6.** 30 Days post-embolization. (a) Clusters of unloaded control beads (yellow arrows) in the distal treated liver, with mild interlobular fibrosis (blue arrows) (x 1 magnification, scale bar = 2 mm). (b) VERB100 beads (yellow arrows) in the intermediate treated liver showing interlobular fibrosis, sometimes encircling reduced size lobules and with bile duct dilatation (red arrow) (x 1 magnification, scale bar = 2 mm). (c) VERB100 beads (yellow arrows) in the portal space, with interlobular fibrosis (blue arrows) and bile duct hyperplasia (green arrows) encircling reduced size lobules (x 4 magnification, scale bar = 500  $\mu$ m). (d) VERB100 beads (yellow arrows) embedded within inflammatory infiltrate within the liver (purple arrow) (x 5 magnification, scale bar = 400  $\mu$ m).

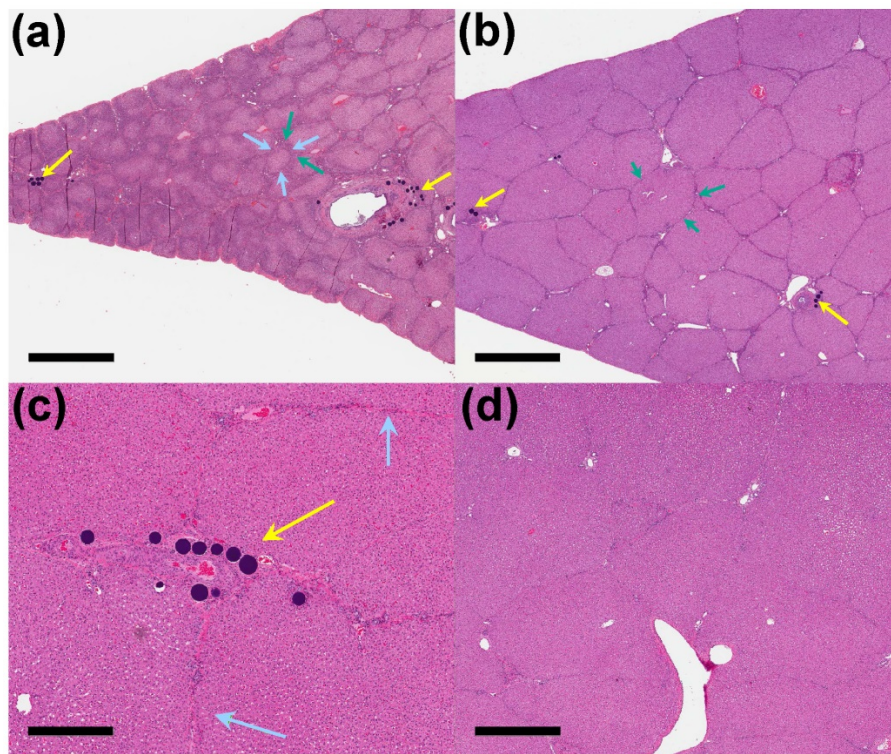


**Figure 7.** 90 Days post-embolization. (a) Unloaded control beads (yellow arrows) with interlobular fibrosis (blue arrows) and bile duct hyperplasia (green arrows) around reduced size lobules (x 1 magnification, scale bar = 2 mm). (b) VERB100 beads (yellow arrows) in the intermediate treated liver with mild bile duct hyperplasia (green arrows) (x 1 magnification, scale bar = 2 mm). (c) VERB100 beads (yellow arrows) integrated into the intermediate treated liver tissue with no signs of reaction or inflammation and mild interlobular fibrosis (blue arrows) (x 4 magnification, scale bar = 500  $\mu$ m). (d) Untreated portion of the liver of an VERB100 group animal for comparison, showing normal connective tissue separating lobules and normal liver tissue appearance (x 2 magnification, scale bar = 1 mm).

The low burst release and  $C_{max}$  observed for VERB can be compared with the reported  $C_{max}$  levels of 42.8-651 ng/mL for doxorubicin loaded DC Bead™ (1 mL administration of 100-300  $\mu$ m and 700-900  $\mu$ m sized beads loaded at 37.5 mg/mL) in a similar embolization model, which typically elutes 0.5-6 % of the loaded dose into the plasma in the first hours post-administration and is considered a slow and sustained release system [36]. This slow *in vivo* release of VTB is attributed to both the radiopaque bead platform, which has a more hydrophobic matrix that retards drug elution, and to the physicochemical properties of the drug, as its solubility is reduced at neutral pH [34]. These properties lead to minimal systemic exposure of drug when delivered from VERB, which is highly desirable when the drug is associated with potential severe adverse cardiac effects when delivered orally at higher doses. [39]

When administered orally, levels of VTB and its metabolites in liver tissue were very high, as anticipated from the daily dosing and long half-life of the drug (19 days in humans). [41] This extended exposure increases the chances of prolonged QT interval, Torsades de pointes and sudden death and why local delivery of lower doses may be a strategy for overcoming these adverse events. When delivered in a locoregional manner *via* the beads, both the phase one and two studies demonstrated measurable levels of VTB and its main metabolite NDM VTB remaining in the liver tissue at 30 days, with much higher levels being found in the targeted embolized than non-embolized tissues. There was no obvious relationship regarding drug levels and location of the tissue sample relative to the point of delivery from the catheter. Most striking was the presence of both VTB and NDM VTB in liver samples at 90 days post administration, which demonstrates the extended release nature of the drug-eluting bead delivery platform. VTB has been shown to be a potent inhibitor of both VEGF-stimulated and EGF-stimulated human umbilical vein endothelial cell (HUVEC) proliferation *in vitro* with reported  $IC_{50}$  levels of 0.06  $\mu$ M and 0.17  $\mu$ M respectively [32]. In this study we observe VTB tissue levels at 30 days in the range 0.073-0.352  $\mu$ M, which demonstrates that this controlled release system should release levels of drug for at least 1 month sufficient to induce the desired anti-angiogenic effects on the tumor vasculature. Moreover, VTB has been shown to elicit a direct inhibition of tumor cell growth, most probably *via* inhibition of EGFR tyrosine kinase activity [42] and may be another mechanism by which locoregional delivery of VTB can induce an antitumor effect.

Despite the increase in density due to the introduction of iodine species to provide radiopacity

[35], VERBs were easily handled by suspension of the 2 mL of hydrated beads in 18 mL of soluble contrast agent, followed by slow administration at a rate of around 1 mL of suspension per minute. The beads could be clearly seen on fluoroscopy as they accumulated in the hepatic vessels and the soluble contrast washed away (Figure 2) [43]. Despite this, some off-target embolization was expected as attempts were made to deliver the full dose of 1 mL of beads, which was achieved in most cases. The radiopacity of the VERB embolic device was shown to be useful not only during delivery for targeting the beads, but at follow-up by CT for identifying bead location and associated imaging findings such as decreased hepatic parenchymal enhancement in the treated locations, embolization-related lobe size reduction and bile duct dilation. Biliary dilatation is likely indicative of hepatic artery ischemia caused by the embolization, because the biliary ducts are supplied by hepatic arteries rather than portal vein blood supply. There was no obvious difference in the radiopacity between VERB with different drug doses used in the phase one study, despite the drug potentially contributing slightly to the overall radiopacity due to the presence of radiodense bromine atoms on the drug structure [34]. The radiopacity of the beads did not change over the 90 day period confirming the stability of the device as demonstrated previously with this radiopaque platform [37].

Based on the histopathological evaluation, there were expected microscopic findings associated with hepatic embolization following intrahepatic administration of up to 1 mL of either the unloaded ROB or VERB100 beads. On day 30, findings in the treated liver of animals administered VERB100 beads consisted of reduced lobule size, bile duct hyperplasia, interlobular fibrosis, and bile duct dilatation/inflammation. By day 90, reduced lobule size and bile duct dilatation/inflammation were resolved in the treated liver sections, whereas bile duct hyperplasia and interlobular fibrosis were still present in the treated sections. On day 90, interlobular fibrosis, reduced lobule size, and/or bile duct hyperplasia were present in the treated liver in the unloaded control group. These findings suggest a more profound effect on the liver parenchyma with VERB100 beads, compared to unloaded control. The study also demonstrated that administration of VERB100 resulted in no obvious systemic toxicity following implantation.

## Conclusions

VTB is a MTKi that has been successfully loaded onto a radiopaque drug-eluting bead platform with

the potential for locoregional administration to treat hepatic malignancies. Different doses of VTB were investigated in the first phase of this study and demonstrated low systemic exposure compared to oral dosing, with a linear relationship between the observed plasma AUC and the dose loaded into the beads. From the second phase of the study it is noted that no unexpected hepatic toxicities were seen, with pathological changes consistent with the effects of embolization of hepatic arterial vasculature, those effects appearing more pronounced when VERBs were delivered into the liver suggesting additional local effects from the drug. One limitation of the swine hepatic artery embolization model is that there is no tumor present and therefore the anti-cancer effects of the drug cannot be properly evaluated. The model does however, offer an indicator of the safety of such an investigational product in a large animal, in which a clinically-relevant dose of drug-loaded bead can be administered and its effects on healthy liver tissue determined. This model has also permitted the quantification of drug and metabolite levels over a sustained period of delivery and coupled with what is already known regarding the efficacy and mode of action of VTB, provides optimism that therapeutic levels of drug may be maintained in the liver over a period of at least a month following treatment. These findings support a First-in-Human evaluation of VERB for the locoregional treatment of hepatic malignancies.

## Abbreviations

MTKi: Multi-tyrosine kinase inhibitor; VERB: Vandetanib-eluting Radiopaque Bead; ROB: Radiopaque Bead; VTB: Vandetanib; TACE: Transarterial chemoembolization;  $C_{max}$ : Peak plasma drug level; AUC: Area under the curve (overall drug exposure); MDCT: Multidetector computed tomography.

## Acknowledgements

The authors would like to thank MPI Research for conducting the embolization procedures and pathological analysis, and York Bioanalytical Solutions Limited for the plasma and tissue analyses of vandetanib and its metabolites.

## Competing Interests

The authors have declared that no competing interest exists.

## References

- [1] Lewis AL, Holden RR. DC Bead embolic drug-eluting bead: clinical application in the locoregional treatment of tumours. *Expert Opin Drug Deliv*. 2011;8:153-69.
- [2] Baltes S, Freund I, Lewis AL, Nolte I, Brinker T. Doxorubicin and irinotecan eluting beads for treatment of glioma - a pilot study in a rat model. *J Mater Sci Mater Med*. 2009;21:1393-402.
- [3] Forster REJ, Small S, Tang Y, Heaysman CL, Lloyd AW, Macfarlane WM, et al. Comparison of DC Bead-Irinotecan and DC Bead-Topotecan Drug Eluting Beads for Use in Locoregional Drug Delivery to Treat Pancreatic Cancer. *J Mater Sci Mater Med*. 2010;21:2683-90.
- [4] Keese M, Gasimova L, Schwenke K, Yagublu V, Shang E, Faissner R, et al. Doxorubicin and mitoxantrone drug eluting beads for the treatment of experimental peritoneal carcinomatosis in colorectal cancer. *Int J Cancer*. 2009;124:2701-8.
- [5] Varela M, Real MI, Burrel M, Forner A, Sala M, Brunet M, et al. Chemoembolization of hepatocellular carcinoma with drug eluting beads: efficacy and doxorubicin pharmacokinetics. *J Hepatology*. 2007;46:474-81.
- [6] Namur J, Citron SJ, Sellers MT, Dupuis MH, Wassef M, Manfait M, et al. Embolization of hepatocellular carcinoma with drug-eluting beads: doxorubicin tissue concentration and distribution in patient liver explants. *J Hepatology*. 2011;55:1332-8.
- [7] Lewis AL. DC Bead(TM): a major development in the toolbox for the interventional oncologist. *Expert Rev Med Devices*. 2009;6:389-400.
- [8] Lammer J, Malagari K, Vogl T, Pilleul F, Denys A, Watkinson A, et al. Prospective randomized study of doxorubicin-eluting-bead embolization in the treatment of hepatocellular carcinoma: results of the PRECISION V study. *Cardiovasc Intervent Radiol*. 2010;33:41-52.
- [9] Malagari K, Pomoni M, Kelekis A, Pomoni A, Dourakis S, Spyridopoulos T, et al. Prospective randomized comparison of chemoembolization with doxorubicin-eluting beads and bland embolization with BeadBlock for hepatocellular carcinoma. *Cardiovasc Intervent Radiol*. 2010;33:541-51.
- [10] Poon RTP, Tso WK, Pang RWC, Ng KKC, Woo R, Tai KS, et al. A Phase I/II Trial of Chemoembolization for Hepatocellular Carcinoma Using a Novel Intra-Arterial Drug-Eluting Bead. *Clin Gastroenterol and Hepatol*. 2007;5:1100-8.
- [11] Aliberti C, Tilli M, Benea G, Fiorentini G. Trans-arterial chemoembolization (TACE) of liver metastases from colorectal cancer using irinotecan-eluting beads: preliminary results. *Anticancer Res*. 2006;26:3793-5.
- [12] Fiorentini G, Aliberti C, Benea G, Del Conte A, Tilli M, Mambrini A. Evaluation at 16 months of a phase III study comparing TACE-DC Beads IRI loaded (DEBIRI) with FOLFIRI (CI) for patients with nonresectable colorectal cancer (CRC) liver metastases (LM). *ASCO 2009 Gastrointestinal Cancers Symposium 2009*.
- [13] Martin RC, Howard J, Tomalty D, Robbins K, Padr R, Bosnjakovic PM, et al. Toxicity of irinotecan-eluting beads in the treatment of hepatic malignancies: results of a multi-institutional registry. *Cardiovasc Intervent Radiol*. 2010;33:960-6.
- [14] Martin RC, Joshi J, Robbins K, Tomalty D, O'Hara R, Tatum C. Transarterial Chemoembolization of Metastatic Colorectal Carcinoma with Drug-Eluting Beads, Irinotecan (DEBIRI): Multi-Institutional Registry. *J Oncol*. 2009;2009:539795.
- [15] Martin RC, Robbins K, Metzger T, O'Hara R, Bosnjakovic P, Tomalty D. Hepatic Intra-arterial Injection of Irinotecan Eluting Beads in Unresectable Colorectal Liver Metastatic Refractory to Standard Systemic Chemotherapy: Results of Mult-institutional Study. *Proc Gastrointestinal Cancers Symp*. 2009;Jan 15-17:152, Abs 85.
- [16] Vinchon-Petit S, Jarnet D, Michalak S, Lewis A, Benoit JP, Menei P. Local implantation of doxorubicin drug eluting beads in rat glioma. *Int J Pharm*. 2010;402:184-9.
- [17] Karaca C, Cizginer S, Konuk Y, Kambadakone A, Turner BG, Mino-Kenudson M, et al. Feasibility of EUS-guided injection of irinotecan-loaded microspheres into the swine pancreas. *Gastrointest Endosc*. 2011;73:603-6.
- [18] Llovet JM, Ricci S, Mazzaferro V, Hilgard P, Gane E, Blanc JF, et al. Sorafenib in advanced hepatocellular carcinoma. *N Engl J Med*. 2008;359:378-90.
- [19] Cheng AL, Kang YK, Chen Z, Tsao CJ, Qin S, Kim JS, et al. Efficacy and safety of sorafenib in patients in the Asia-Pacific region with advanced hepatocellular carcinoma: a phase III randomised, double-blind, placebo-controlled trial. *Lancet Oncol*. 2009;10:25-34.
- [20] Philip PA, Mahoney MR, Allmer C, Thomas J, Pitot HC, Kim G, et al. Phase II study of Erlotinib (OSI-774) in patients with advanced hepatocellular cancer. *J Clin Oncol*. 2005;23:6657-63.
- [21] Autier J, Escudier B, Wechsler J, Spatz A, Robert C. Prospective study of the cutaneous adverse effects of sorafenib, a novel multikinase inhibitor. *Arch Dermatol*. 2008;144:886-92.
- [22] Kong HH, Turner ML. Array of cutaneous adverse effects associated with sorafenib. *J Am Acad Dermatol*. 2009;61:360-1.
- [23] Lee WJ, Lee JL, Chang SE, Lee MW, Kang YK, Choi JH, et al. Cutaneous adverse effects in patients treated with the multitargeted kinase inhibitors sorafenib and sunitinib. *Br J Dermatol*. 2009;161:1045-51.
- [24] Fuchs K, Bize PE, Denys A, Borchard G, Jordan O. Sunitinib-eluting beads for chemoembolization: methods for in vitro evaluation of drug release. *Int J Pharm*. 2015;482:68-74.
- [25] Fuchs K, Bize PE, Dormond O, Denys A, Doelker E, Borchard G, et al. Drug-eluting beads loaded with antiangiogenic agents for chemoembolization: in vitro sunitinib loading and release and in vivo pharmacokinetics in an animal model. *J Vasc Intervent Radiol*. 2014;25:379-87, 87 e1-2.

- [26] Bize P, Duran R, Fuchs K, Dormond O, Namur J, Decosterd LA, et al. Antitumoral Effect of Sunitinib-eluting Beads in the Rabbit VX2 Tumor Model. *Radiology*. 2016;280:425-35.
- [27] Cheng AL, Kang YK, Lin DY, Park JW, Kudo M, Qin S, et al. Sunitinib versus sorafenib in advanced hepatocellular cancer: results of a randomized phase III trial. *J Clin Oncol*. 2013;31:4067-75.
- [28] Chau NG, Haddad RI. Vandetanib for the treatment of medullary thyroid cancer. *Clin Cancer Res*. 2013;19:524-9.
- [29] Degrauwe N, Sosa JA, Roman S, Deshpande HA. Vandetanib for the treatment of metastatic medullary thyroid cancer. *Clin Med Insights Oncol*. 2012;6:243-52.
- [30] Deshpande H, Roman S, Thumar J, Sosa JA. Vandetanib (ZD6474) in the Treatment of Medullary Thyroid Cancer. *Clin Med Insights Oncol*. 2011;5:213-21.
- [31] Ton GN, Banaszynski ME, Kolesar JM. Vandetanib: a novel targeted therapy for the treatment of metastatic or locally advanced medullary thyroid cancer. *Am J Health Pharm*. 2013;70:849-55.
- [32] Ryan AJ, Wedge SR. ZD6474--a novel inhibitor of VEGFR and EGFR tyrosine kinase activity. *Br J Cancer*. 2005;92 Suppl 1:S6-13.
- [33] Hsu C, Yang TS, Huo TI, Hsieh RK, Yu CW, Hwang WS, et al. Vandetanib in patients with inoperable hepatocellular carcinoma: a phase II, randomized, double-blind, placebo-controlled study. *J Hepatology*. 2012;56:1097-103.
- [34] Hagan A, Phillips GJ, MacFarlane WM, Lloyd AW, Czuczman P, Lewis D. Preparation and Characterization of Vandetanib-eluting Radiopaque Beads for Locoregional Treatment of Hepatic Malignancies. *Eur J Pharm Sci*. 2017;101:22-30.
- [35] Duran R, Sharma K, Dreher MR, Ashrafi K, Mirpour S, Lin M, et al. A Novel Inherently Radiopaque Bead for Transarterial Embolization to Treat Liver Cancer - A Pre-clinical Study. *Theranostics*. 2016;6:28-39.
- [36] Lewis AL, Taylor RR, Hall B, Gonzalez MV, Willis SL, Stratford PW. Pharmacokinetic and safety study of doxorubicin-eluting beads in a porcine model of hepatic arterial embolization. *J Vasc Interv Radiol*. 2006;17:1335-43.
- [37] Sharma KV, Bascal Z, Kilpatrick H, Ashrafi K, Willis SL, Dreher MR, et al. Long-term biocompatibility, imaging appearance and tissue effects associated with delivery of a novel radiopaque embolization bead for image-guided therapy. *Biomaterials*. 2016;103:293-304.
- [38] Agency EM. Caprelsa Assessment Report. European Medicines Agency; 2011:1-88.
- [39] AstraZeneca. Vandetanib (ZD6474) Tablets. Oncologic Drugs Advisory Committee (ODAC) Meeting Briefing Document; 2010:1-71.
- [40] Thornton K, Kim G, Maher VE, Chattopadhyay S, Tang S, Moon YJ, et al. Vandetanib for the treatment of symptomatic or progressive medullary thyroid cancer in patients with unresectable locally advanced or metastatic disease: U.S. Food and Drug Administration drug approval summary. *Clin Cancer Res*. 2012;18:3722-30.
- [41] Research CfDEa. Clinical Pharmacology and Pharmaceutics Review: 022405Orig1s000: Vandetanib. Food and Drug Administration; 2010.
- [42] Arao T, Fukumoto H, Takeda M, Tamura T, Saijo N, Nishio K. Small in-frame deletion in the epidermal growth factor receptor as a target for ZD6474. *Cancer Res*. 2004;64:9101-4.
- [43] Levy EB, Krishnasamy VP, Lewis AL, Willis S, Macfarlane C, Anderson V, et al. First Human Experience with Directly Image-able Iodinated Embolization Microbeads. *Cardiovasc Intervent Radiol*. 2016;39:1177-86.